Preparation and Characterization of Nanocellulose from Beer Industrial Residues Using Acid Hydrolysis/Ultrasound

Article *in* Fibers and Polymers · April 2015

DOI: 10.1007/s12221-015-0529-4

CITATIONS
21

READS
382

4 authors:

Iman Shahabi-Ghahfarrokhi
University of Zanjan
19 PUBLICATIONS **190** CITATIONS
SEE PROFILE

Faramarz Khodaiyan
University of Tehran
86 PUBLICATIONS **1,286** CITATIONS
SEE PROFILE

Mohammad Mousavi
University of Tehran
228 PUBLICATIONS **3,935** CITATIONS
SEE PROFILE

Hossein Yousefi
Gorgan University of Agricultural Sciences and Natural Resources
34 PUBLICATIONS **559** CITATIONS
SEE PROFILE

Fibers and Polymers 2015, Vol.16, No.3, 529-536
DOI 10.1007/s12221-015-0529-4

ISSN 1229-9197 (print version)
ISSN 1875-0052 (electronic version)

Preparation and Characterization of Nanocellulose from Beer Industrial Residues Using Acid Hydrolysis/Ultrasound

Iman Shahabi-Ghahafarrokhi*, Faramarz Khodaiyan[1], Mohammad Mousavi[1], and Hossein Yousefi[2]

Department of Food Science and Technology, Faculty of Agriculture, University of Zanjan, Zanjan 38791-45371, Iran
[1]Department of Food Science and Engineering, Campus of Agriculture and Natural Resources, University of Tehran, Karaj 31587-77871, Iran
[2]Department of Wood Engineering and Technology, Gorgan University of Agricultural Sciences and Natural Resources, Gorgan 49138-15739, Iran

(Received May 22, 2014; Revised October 26, 2014; Accepted November 9, 2014)

Abstract: The aim of this work was to prepare nanocellulose (NC) from beer industrial residuals (BIR) by an acid hydrolysis/ultrasound method using three hydrolysis times (2, 4, and 6 hours). The atomic-force micrographs showed that the obtained NCs had whisker, oval, and spherical shapes. The average diameters of the NCs ranged between 73 and 146 nm. The chemical characterization of BIR and purified cellulose confirmed that α-cellulose content increased from 44 % to 92 % and lignin contents decreased from 32 % to 5 %. FT-IR analysis showed a substantial change in chemical structure of NCs (especially over the 2-hour hydrolysis time) compared to that of purified BIR fibers. XRD results revealed that the NCs' crystallinity and crystallite size were positively affected by acid-hydrolysis time. TGA results showed that the thermal stability of NCs increased as a result of hydrolysis. BIR, a low-value residue, was turned to nanocellulose, a high-performance nanomaterial.

Keywords: Beer industrial residues, Barley, Nanocellulose, Acid hydrolysis, Ultrasound

Introduction

Growing awareness of ecological, social, and economic issues, the high rate of depletion of petroleum resources, concepts of sustainability, and new environmental regulations have stimulated the search for green materials compatible with the environment. Cellulose is abundantly present in plants such as grasses, reeds, stalks, and woody vegetation, as well as in bacteria [1]. Cellulose, composed of nanostructures including crystals, elementary fibrils, and nanofibrils, is a linear homopolymer of D-glucopyranose units linked by β-1,4-glycosidic bonds ($C_{6n}H_{10n+2}O_{5n+1}$ (n=degree of polymerization of glucose)). The main advantages of cellulose nanostructures as raw materials are their abundance, low cost, low density, biocompatibility, non-toxicity, biodegradability, low coefficient of thermal expansion, high specific strength, and high modulus [2,3]. Functional hydroxyl groups in cellulose make it a highly reactive material, thus, cellulose can be chemically modified for further applications [2-4]. All these features make cellulose a very promising material for nanotechnology.

Cellulose nanostructures are isolated through several top-down approaches including mechanical treatments such as cryocrushing [5], ultra-fine friction grinding [6,7], high-pressure homogenizing [8], chemical treatments such as acid hydrolysis [4,9], ultrasound [9,10], enzyme-assisted hydrolysis [11], TEMPO-mediated oxidation [12], and solvent-assisted isolation [13]. Two or more of these methods have also been combined to produce different types of nanostructure cellulose.

*Corresponding author: i.shahabi@ut.ac.ir

Acid hydrolysis is the oldest isolation method of cellulose nanostructures, it produces rod-like, high-crystalline cellulose nanowhiskers. Wide varieties of cellulose resources such as canola straw [7], cotton [9], wheat straw [4,14], soy hull [5], banana fiber [15], bagasse sugarcane [16], bio-residues of wood bioethanol production [17], and wood powder [10] have been used to produce nanocellulose (NC). In the current study, we used beer-husk residues, or beer industrial residues (BIR), after wort separation to produce NC. According to FAO statistics, about 8.3 million metric tons of barley seeds were cropped worldwide in 2010 [18]. During this time, over 179 million metric tons of beer were produced [19]. Thus, it is worth trying to convert this abundant food-industry by-product into high-performance materials. The aim of this work was to isolate and characterize NC from BIR using acid hydrolysis coupled with high-intensity ultrasound.

Experimental

Materials

BIR was collected from Behnoush Iran Co., Iran. Analytical-grade chemicals, including sodium hydroxide (NaOH), potassium hydroxide (KOH), acetic acid (CH_3COOH), acetone (CH_3COCH_3), and hydrochloric acid (HCl), were purchased from Dr. Mojallai Co., Iran. Sodium chlorite ($NaClO_2$) was provided by Fluka Chemical Co., Germany.

Cellulose Purification

Raw BIR suspension (10 %) was boiled for 1 hour and dried at 105 ^{o}C to constant weight. Then the slury (10 %) of dried BIR in NaOH (2 %) was soaked overnight. The soaked

BIR was washed with water, then treated with 12 % NaOH at 121 °C by autoclave for 45 minutes (three times) to produce BIR pulp. The BIR pulp was washed, and then dried at 105 °C. For removing residual lignin, the pulp slurry with consistency of 5 wt% was treated twice by a solution containing 3 % $NaClO_2$ and 1.5 % CH_3COOH at 75 °C for 1 hour. To remove hemicelluloses, the treated pulp was soaked in a 3 % KOH solution overnight, followed by treating at 80 °C for 1 hour. The pulp was further bleached using 3 % $NaClO_2$ and 1.5 % CH_3COOH at 75 °C for 1 hour. Finally, the purified BIR cellulose was dried at 105 °C.

Preparation of NC

The slurry of dried purified BIR cellulose to 10 % HCl was hydrolyzed at 80 °C for 2, 4, and 6 hours [14]. The hydrolyzed cellulose was washed three times by centrifugation (Mikro 200, Hettich, Germany) at 6000 rpm, 4 °C for 30 min. Next, to remove residual acid and neutralize the pH, a dialysis tube (Sigma Aldrich, Germany) soaked in distillated water was used. To disperse coagulated neutralized cellulose particles, ultrasonic treatment (Hielscher UP200S, Germany) for 15 minutes sessions resulted in NCs. The NCs prepared with 2, 4, and 6 hours hydrolysis times are hereafter referred as to NC-2, NC-4, and NC-6, respectively.

Measurements

Suspension Stability

The stability of a 0.2 % suspension of purified BIR fibers and NCs prepared with different hydrolysis times was checked over time using a digital camera (ELPH 100 HS, Canon, Japan).

Morphology

A scanning electron microscope (SEM, CamScan MV2300, Electron Optic Services, Canada) was used for microstructural analysis of BIR fibers. Specimens were coated with gold prior to taking micrographs at an accelerating voltage of 15 kV.

An atomic-force microscope (AFM, DualscopeC26, DME, Denmark) was used to take micrographs of the NCs. The specimens were placed onto freshly cleaved mica and left to dry at room temperature prior to scanning.

The dimensions of the BIR fibers and NCs were measured on SEM and AFM micrographs respectively, using an UTHSCSA Image Tool (University of Texas Health Science Center, USA).

Chemical Characterization of NC

The α-cellulose content (ACC) of specimens was determined according to the TAPPI T 203 cm-99 standard [20]. 1.5 g (W_1, dry weight) of fiber sample was stirred in 100 m*l* NaOH (17.5 %) for 30 min. Distilled water (100 m*l*) was then added to dilute the NaOH. The dilute mixture was left to stir for 30 min. After stirring, the cellulose fractions were collected by filtering, followed by drying at 105 °C (W_2). Three replications of each specimen were used for calculating α-cellulose content (equation (1)).

$$ACC\ (\%) = \frac{W_2}{W_1} \times 100 \quad (1)$$

The acid-insoluble lignin of specimens was determined according to TAPPI T 222 om-98 standard [21]. Two grams dried specimen (W_1) were added to 15-40 m*l* sulfuric acid (72 %) and stirred at 20 °C for 2 h. The mixture was then added to 575-1540 m*l* distilled water and boiled using a reflux condenser. Next, the precipitant was removed by filtration and washed with hot water until it was acid-free. Finally, the residual acid-insoluble lignin (AIL) was weighed (W_4), and the acid-insoluble content was calculated with three replications (equation (2)).

$$AIL\ (\%) = \frac{W_4}{W_1} \times 100 \quad (2)$$

The ash content of specimens was determined according to TAPPI T 211om-93 standard [22]. At least one gram of dried specimen (W_1) were transferred to cleaned crucible and made to ash at 525±25 °C. Finally, the residual ash was weighted (W_5), and ash combustion at 525 (A) was calculated with three replications (equation (3))

$$A\ (\%) = \frac{W_5}{W_1} \times 100 \quad (3)$$

X-ray Diffraction

X-ray diffraction (XRD) profiles of pure BIR fibers and NCs prepared with different hydrolysis times were taken using a Bruker Advance D8 (Karlsruhte, Germany). The samples in powdered form were irradiated by Cu K_α (λ= 0.15418 nm) at 40 kV and 30 mA with a symmetric reflection geometry in the range of 2θ=10-40 ° with a step of 0.02 °. The crystallinity index (CrI) of the specimens was evaluated by the method of Segal and coworkers [23] (equation (4)).

$$C_{rI}\ (\%) = 100 \times \left[\frac{I_{002} - I_{am}}{I_{002}}\right] \quad (4)$$

where I_{002} is the intensity of [002] reflection (2θ=21-23 °) and I_{am} is the intensity of amorphous cellulose (2θ=18 °).

The crystallite size of cellulose was also estimated by Scherrer's equation (equation (5))

$$D = \frac{\lambda}{\beta \cos\theta} \quad (5)$$

where D is the crystallite size, λ is the X-ray wavelength (0.15418 nm), θ is the diffraction angle for the [002] plane, and β is the corrected integral width [7].

FT-IR

The IR spectrum of specimens was determined using a Fourier transform Infra-Red (FT-IR) spectrometer (IRPrestige-21, Shimadzu, Japan). The specimens were ground with KBr powder and pressed into pellets for FT-IR measurement in the wave-number range of 4000-400 cm^{-1} at a resolution of 4 cm^{-1}.

Thermogravimetric Analysis (TGA)

The thermal-degradation characteristics of BIR fibers and different NCs were analyzed using a TGA Q 50 series thermogravimetric (TA instrument, USA) in a nitrogen atmosphere condition. Specimens of three to six milligrams were loaded for each measurement in duplicate, and then heated from room temperature to 700 °C at a rate of 10 °C/min. The results were reported in percent of weight lost and weight-loss derivative versus temperature.

Results and Discussion

Suspension Stability

Figure 1 shows the suspension stability of purified BIR fibers and NC after 100 min. The stability of the NC suspension was drastically greater than that of the fiber suspension. Furthermore, the stability of NC increased with longer hydrolysis time. This is because the specific surface area, the amount of electro-statistical repulsion, and the accident Brownian movement of nano particles in NC suspension are much higher than those for a fiber suspension.

Chemical Characterization of NC

Table 1 presents the chemical comparison of BIR before and after purification. Lignin was effectively removed by chemical treatments. This is why the ratio of α-cellulose of BIR fibers (44 %) drastically increased to 92 % while lignin content decreased. The yield of NC-2, NC-4 and NC-6 was 27.6, 25.5 and 24.4 %. The efficiency of current method is comparable with previous researchers [24,25].

Morphology

Figures 2(a) and 2(b) show the SEM micrographs of BIR fibers (a) before and (b) after purification. The microstructure of BIR fibers could not be clearly observed prior to pulping

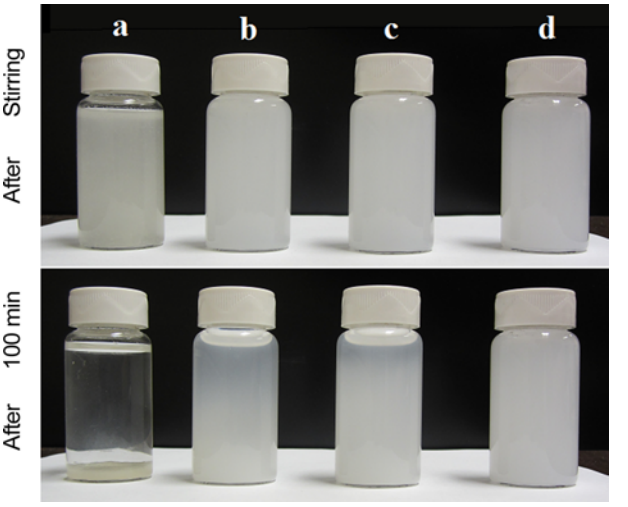

Figure 1. Suspension stability of BIR (a) purified cellulose, (b) NC-2, (c) NC-4, and (d) NC-6.

Table 1. Chemical composition of BIR before and after cellulose purification

BIR fibers	α-cellulose (%)	Total lignin (%)	Ash (%)
Untreated BIR fibers	43.79±2.36	26.62±1.13	4.03±0.24
Purified BIR fibers	91.81±1.19	3.21±0.37	1.67±0.45

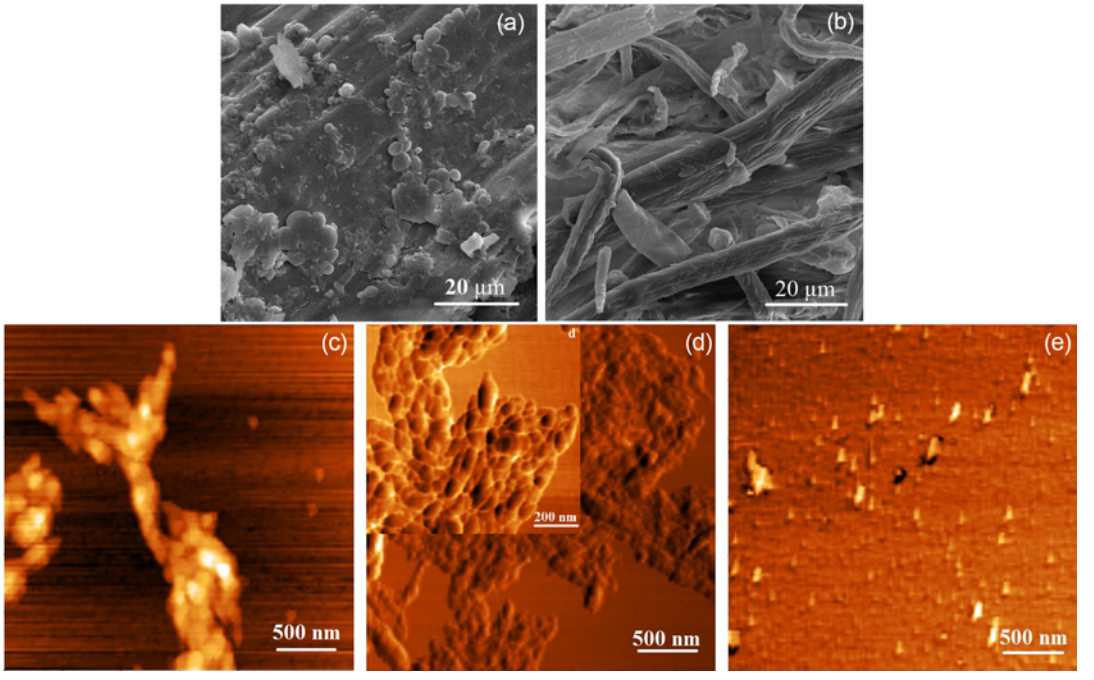

Figure 2. SEM micrograph of BIR cellulose fibers (a) before and (b) after cellulose purification, AFM micrographs of (c) NC-2, (d) NC-4, and (e) NC-6.

and bleaching; however, the fibers were separately seen after purification. This is because lignin and other impurities were removed through chemical purification.

Figure 2(c to e) shows the AFM micrographs for NC-2, NC-4, and NC-6. Microscale cellulose fibers from BIR were successfully downsized to nanoscale thorough acid hydrolysis. Cellulose nanostructures (whiskers, and whisker-to-ovular, and spherical shapes) were observed in the AFM micrographs of NC-2 and NC-4, while that of NC-6 did not show nanocomponents clearly. It seems the dimension of whiskers drastically decreased as the result of long acidic treatment; hence, the nanocomponents could not be clearly observed by AFM.

Figure 3 presents the average diameter, length and

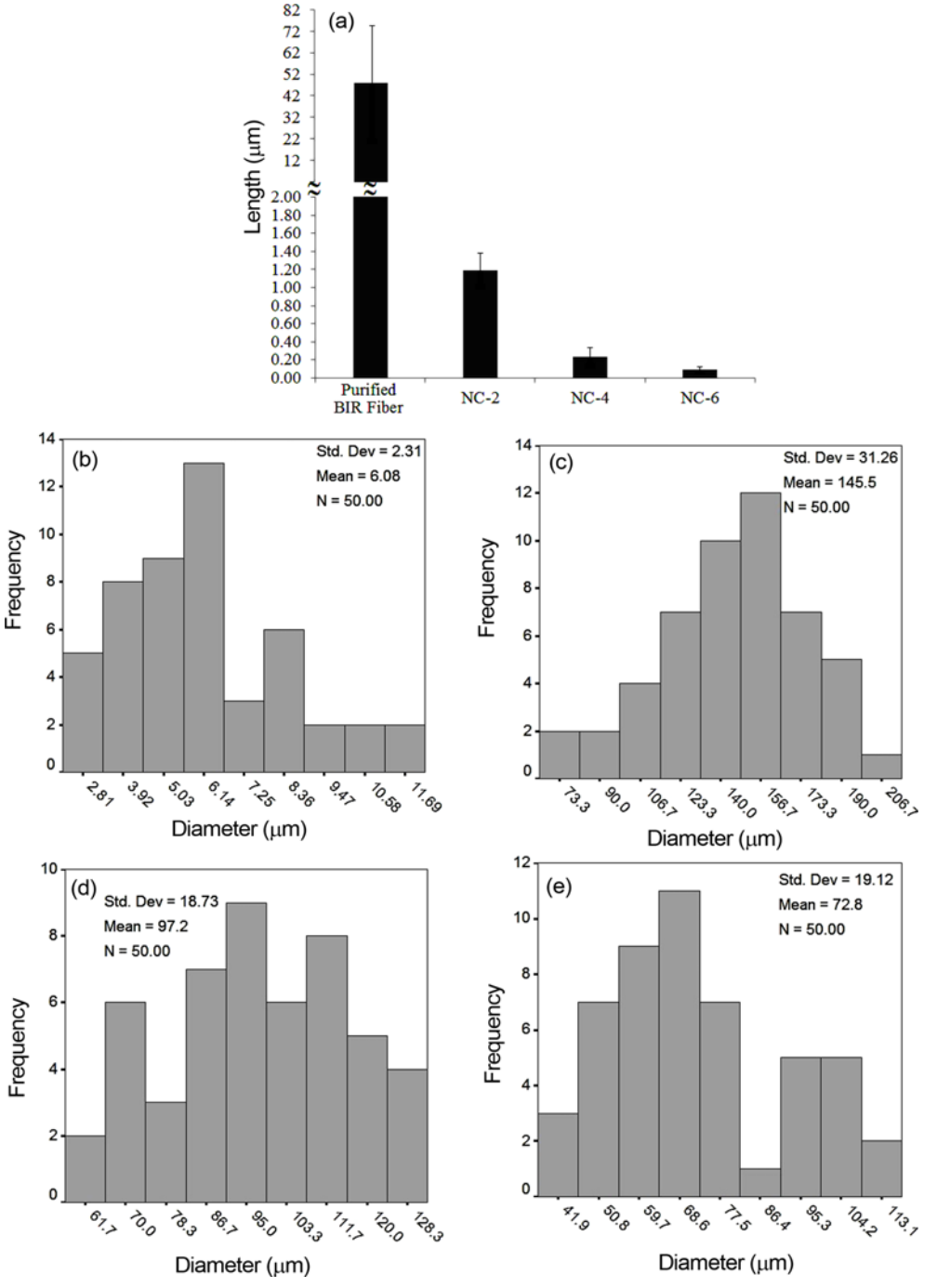

Figure 3. (a) Length average of BIR purified cellulose and NCs prepared with different hydrolysis times; diameter average and distribution of (b) BIR purified cellulose, (c) NC-2, (d) NC-4, and (e) NC-6.

distribution of BIR purified fibers and NCs prepared with different hydrolysis times. The length of the BIR fiber was 47.89±26.82 μm (Figure 3(a)). The average length of NC-2, NC-4, and NC-6 decreased drastically to 1.19±0.18 μm, 0.23±0.10 μm, and 0.10±0.02 μm, respectively. The diameter of the BIR fibers was 6.1±2.3 μm (Figure 3(b)). After acidic treatments, the corresponding diameter of NC-2, NC-4, and NC-6 drastically decreased to 146±31 nm, 97±19 nm, and 73±19 nm, respectively.

X-ray Diffraction

Figure 4 shows the X-ray diffraction profiles of BIR fibers and NCs prepared with different hydrolysis times. Table 2 presents the crystallite size and crystallinity of BIR fibers and NCs prepared with different hydrolysis times. The XRD profiles of purified BIR fibers and NCs prepared with different hydrolysis times showed cellulose I_β peaks at 2θ= 15, 16.5, 20.1, 22.5, and 35.2 degree, which could be attributed to [101], [10$\bar{1}$], [021], [002] and [040] atomic planes, respectively [26]. However, the origin of the new peak appeared at 2θ of 12.1 degree just in XRD profiles of NCs was unknown, which was also reported by Pullawan et al., 2010 [27]. The strongest peak appeared around 2θ= 22.5 degree was considered for the measurement of crystallinity and crystallite size. The longer hydrolysis time caused narrower and sharper peaks. This is judged from X-ray diffraction profiles, as shown in Figure 4, and FWHM (full width of the diffraction peak measured at half maximum height), as presented in Table 2. The crystallinity and crystallite size of specimens were positively affected by hydrolysis

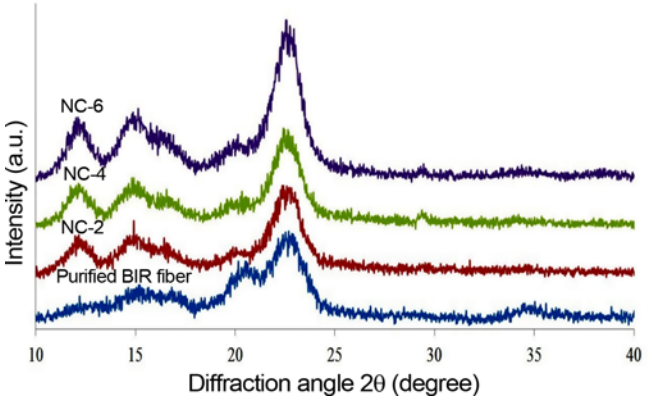

Figure 4. XRD profiles of BIR fibers and NCs prepared with different hydrolysis times.

times. On the other hand, with the increase of hydrolysis time, non-crystalline scattering (around 2θ=18 degrees) apparently vanished, whereas two broad peaks appeared at around 2θ=12.1 and 14.8 degrees. These are attributed to the fact that with the increase in hydrolysis time, the acid destroyed the amorphous phase and left a higher portion of the crystalline phase (Table 2). These results are compatible with the literature [4,14]. The crystallite size increased as the result of acid hydrolysis. This is because acid destroyed the thinner crystallites and less-ordered phases, resulting in a thicker crystallite size on average and a narrower crystallite-size distribution. Re-crystallization may also be an alternative reason for the slight increase of crystallite size during NC production [28].

FT-IR

The FT-IR spectra of purified BIR fibers and NCs are shown in Figure 5. The broad spectrum from 3700-3100 cm^{-1} contains the fundamental stretching modes of hydroxyl groups (O-H) due to carbohydrates and vibrations of the hydrogen bonded hydroxyl groups [4,14,29]. The spectrum from 3000-2800 cm^{-1} could be attributed to the symmetric and anti-symmetric stretching modes of C-H in methyl (CH_3) and methylene (CH_2) functional groups [29,30]. The peaks at 2902 cm^{-1} were due to the aliphatic saturated C-H stretching vibration in cellulose [4]. The peak around 1640 cm^{-1} was assigned to C=C stretching band and associated with the adsorbed water [14,30]. The spectrum from 1500-1300 cm^{-1} was attributed to the C-H bending bands [30]. After acid hydrolysis, the peak at 1325 cm^{-1} was eliminated in NCs. The peak at 1325 cm^{-1} was attributed to S ring (CH_2 rocking at C6 in cellulose) [29]. It seems, the developed hydrogen-bonding network in crystalline structure of NCs, decreased the rocking movement of CH_2. 1200-950 cm^{-1} a broad and intense band which holds the peaks was mainly assigned to stretching modes of carbohydrate rings and side group (C-O-C, C-OH, C-H) [29,30]. The peak at 896 cm^{-1} indicated the typical structure of cellulose (due to β-glycosidic linkages of glucose ring of cellulose) and C-H rocking vibrations of cellulose [4,14].

Thermogravimetric Analysis

In general, the thermolysis reaction of cellulose occurred by the cleavage of glycoside bonds, C-H, C-O, C-C bonds, and by dehydration, decarboxylation and decarbonilation [31].

Figure 6(a) and Figure 6(b) show the thermogravimetric

Table 2. Bragg angle, FWHM, crystallite size and crystallinity index of BIR fiber and NCs prepared with different hydrolysis times

Cellulose structure	Bragg angle (degree)	FWHM (degree)	Crystallite size (nm)	Crystallinity index (%)
Purified BIR fibers	11.34	2.2165	4.06	72.17
NC-2	11.18	1.6356	5.51	79.13
NC-4	11.21	1.6358	5.51	85.40
NC-6	11.27	1.5452	5.83	89.97

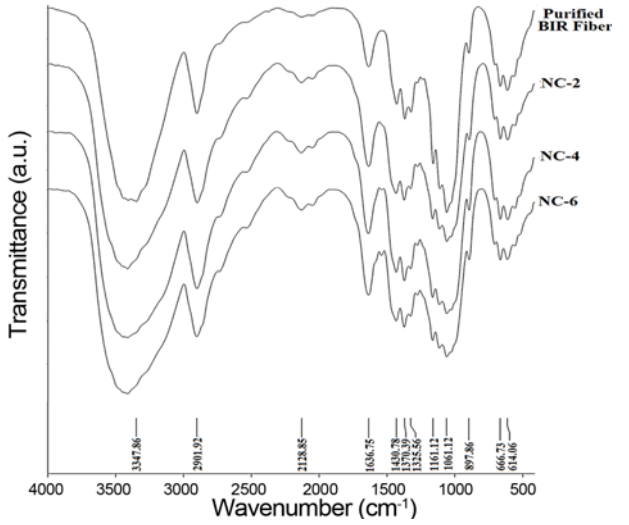

Figure 5. FT-IR spectra of BIR fibers and NCs prepared with different hydrolysis times.

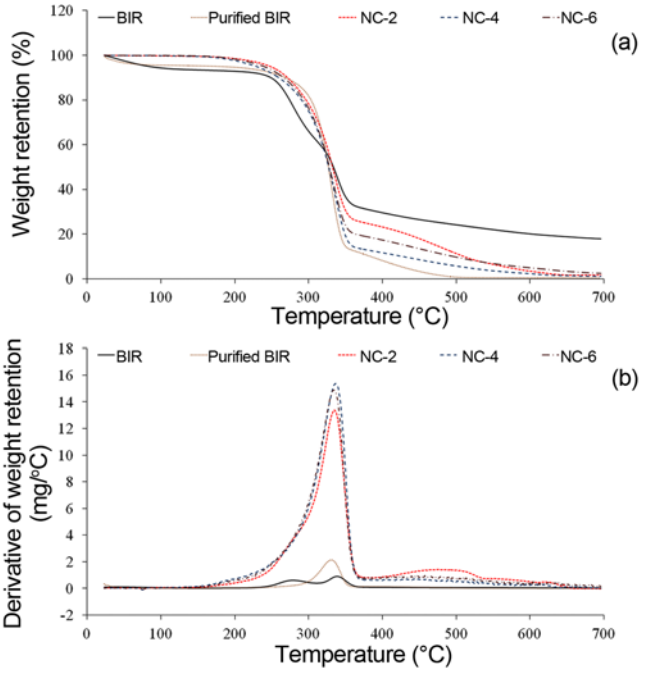

Figure 6. (a) TG and (b) DTG curves of BIR, BIR purified cellulose and NCs prepared with different hydrolysis times.

(TG) and derivative TG (DTG) results for BIR, purified BIR, and NCs prepared with different hydrolysis times. The TG curve (Figure 6(a)) shows the weight loss of NC specimens during thermal processing. This property is useful to evaluate the thermal stability of NCs during composition with polymers commonly used in packaging. In contrast, DTG curves (Figure 6(b)) show the maximum thermal degradation temperature (MTD); in other words, the critical temperature for preparing NC-polymer nanocomposites. The MTD and residual mass (RM) after TGA analysis are also presented in Table 3.

As depicted in Figure 6(b), the DTG of BIR showed two wide and flat peaks with a gently sloping baseline at 278 °C and 336 °C, which is a typical TGA curve of the lignocellulosic specimen [32,33]. The DTG peaks at 278 °C and 336 °C originated from lignin and cellulose degradation, respectively [32,33]. Furthermore, the DTG of purified BIR showed a wide peak with a gently sloping base line at 334 °C. It seems this is attributed to heterogeneous-amorphous and crystalline region-structure of purified BIR. It brought about a broad peak with a gently sloping baseline.

During cellulose purification, a considerable amount of inorganic compounds were removed from BIR. Hence, there was a significant difference between the RM of BIR and the other specimens (Table 3). The RM of specimens is deeply dependence on the nature of specimen and the condition of TGA [32,34].

As shown in Table 3, there was no significant difference between MTD of the BIR and purified BIR. Although the structure of purified cellulose is more heat-stable than crude cellulose [14,31], the high inorganic residual of BIR (Table 3) increased the ratio of heat resistance compound, simultaneously. On the other hand, as shown in Figure 6(b), the thermal degradation of BIR started from less than 300 °C. It can be concluded that the thermal stability of BIR was lower than purified BIR. Notwithstanding, previous studies showed that the thermal stability of lignocellulosic compounds strongly depended on purification method, the ratio of delignificating agents to lignocellulosic compounds, and the nature of the lignocellulosic compounds [14,32].

A sharp peak appeared in DTG curve of NCs. It may be due to high cellulose content and homogeneity of the crystalline structure of NCs. These results showed that the thermal stability of NCs was significantly more than purified BIR, but there was no significant difference between those

Table 3. Thermal-degradation properties of BIR, purified BIR and NCs prepared with different hydrolysis times

Specimen	MTD[a] (°C)	Weight loss at MTD (%)	50 % weight loss temperature (°C)	Residual mass (%)
BIR	336.62±2.78ab	47.37±2.39a	333.26±0.36b	16.04±2.62a
Purified BIR	334.93±1.71b	41.74±0.25b	331.02±1.47b	0.67±0.26b
NC-2	341.38±1.83a	45.25±2.37ab	337.55±0.29a	1.61±0.01b
NC-4	340.59±1.63a	37.06±0.78c	332.01±1.28b	1.32±0.30b
NC-6	339.21±1.28a	42.90±0.59b	333.38±0.80b	1.73±0.66b

[a]Maximum thermal degradation temperature.

of NCs. This result is in accord with previous studies [4,14]. These results revealed a relationship between the structure and the thermal degradation of cellulose. A greater crystalline structure required a higher degradation temperature [4]. While there are no relevant studies of barley base NC, the thermal stability of BIR-base NC is comparable with extracted cellulose from barley straw [31], and NCs produced from other sources [4,14]. These results are consistent with XRD and FT-IR results.

Conclusion

In this study, BIR, a low-value waste byproduct of the food industry, was turned into a high-value-added nanomaterial (nanocellulose). AFM images confirmed NCs diameter ranged from 73 to 145 nm. FT-IR and XRD studies evidenced about the dissolution of lignin and hemicellulose with chemical treatment of the fibers, which resulted in improved thermal stability. Reducing NCs diameters improved the stability of NCs suspension up to 24 h. The results of characterization confirmed that the properties of BIR nanocellulose are in the range of those prepared from other sources, as reported in the literature. The average yield of NC production was 25.8 %. However the performance of this method is not good but it is in the range of acid hydrolysis method. BIR nanocellulose is regarded as a multi-functional material with a wide variety of potential applications including paper and packaging, paints, medical engineering, cosmetics, and defense.

Acknowledgements

The authors are grateful to the University of Tehran and the Iranian Nanotechnology Council, which provided financial aid for this research. They would also like to thank Mahar Fan Abzar Co. for the preparation of AFM micrographs. We would like to acknowledge the extraordinary suggestions and technical support of Professor Babak Ghanbarzadeh and Dr. Habib Kazemi.

References

1. S. Thomas, S. A. Paul, L. A. Pothan, and B. Deepa, in "Cellulose Fibers: Bio- and Nano-polymer Composites" (S. Kalia, B. S. Kaith, and I. Kaur Eds.), pp.3-37, Berlin, Springer, 2011.
2. M. A. S. Azizi Samir, F. Alloin, and A. Dufresne, *Biomacromolecules,* **6**, 612 (2005).
3. H. Abdul Khalil, A. H. Bhat, and A. F. Ireana Yusra, *Carbohydr. Polym.*, **87**, 963 (2012).
4. A. Kaushik and M. Singh, *Carbohydr. Res.,* **346**, 76 (2011).
5. A. Alemdar and M. Sain, *Compos. Sci. Technol.,* **99**, 557 (2008).
6. T. Taniguchi and K. Okamura, *Polym. Int.,* **47**, 291 (1998).
7. H. Yousefi, M. Faezipour, T. Nishino, A. Shakeri, and G. Ebrahimi, *Polymer,* **43**, 559 (2011).
8. M. Jonoobi, J. Harun, P. M. Tahir, A. Shakeri, S. Saiful Azry, and M. Davoodi Makinejad, *Mater. Lett.,* **65**, 1098 (2011).
9. M. Roohani, Y. Habibi, N. M. Belgacem, G. Ebrahim, A. N. Karimi, and A. Dufresne, *Eur. Polym. J.,* **44**, 2489 (2008).
10. W. Chen, H. Yu, Y. Liu, P. Chen, M. Zhang, and Y. Hai, *Carbohydr. Polym.,* **83**, 1804 (2011).
11. N. Hayashi, T. Kondo, and M. Ishihara, *Carbohydr. Polym.,* **61**, 191 (2005).
12. T. Saito, Y. Nishiyama, J.-L. Putaux, M. Vignon, and A. Isogai, *Biomacromolecules,* **7**, 1687 (2006).
13. H. Yousefi, T. Nishino, M. Faezipour, G. Ebrahimi, and A. Shakeri, *Biomacromolecules,* **12**, 4080 (2011).
14. A. Alemdar and M. Sain, *Bioresour. Technol.,* **99**, 1664 (2008).
15. B. Deepa, E. Abraham, B. Mathew Cherian, A. Bismarck, J. J. Blaker, L. A. Pothan, A. Lopes Leao, S. Ferreira de Souza, and M. Kottaisamy, *Bioresour. Technol.,* **102**, 1988 (2011).
16. D. Bhattacharya, L. T. Germinario, and W. T. Winter, *Carbohydr. Polym.,* **73**, 371 (2008).
17. M. A. Herrera, A. P. Mathew, and K. Oksman, *Mater. Lett.,* **71**, 28 (2012).
18. FAO, "FAOSTAT", 2013. [Online]. Available: http://faostat.fao.org/site/567/DesktopDefault.aspx?PageID=567#ancor.
19. FAO, "FAOSTAT", 2013. [Online]. Available: http://faostat.fao.org/site/636/DesktopDefault.aspx?PageID=636#ancor.
20. TAPPI, "Alpha-, beta- and gamma-cellulose in pulp, T 203 cm-99", Chemical Properties Committee of the Process and Product Quality Division, pp.1-5, 1999.
21. TAPI, "Acid-insoluble Lignin in Wood and Pulp, T 222 om-98", Chemical Properties Committee of the Process and Product Quality Division, pp.1-5, 1998.
22. TAPI, "Ash in Wood, Pulp, Paper and Paperboard: Combustion at 525 ^{o}C, T 211 om-93", Chemical Properties Committee of the Process and Product Quality Division, pp.1-4, 1993.
23. L. Segal, J. J. Creely, A. E. J. Martin, and C. M. Conrad, *Text. Res. J.,* **29**, 786 (1959).
24. D. Bondeson, A. Mathew, and K. Oksman, *Cellulose,* **13**, 171 (2006).
25. Y. M. Zhou, S. Y. Fu, L. M. Zheng, and H. Y. Zhan, *Express Polym. Lett.,* **6**, 794 (2012).
26. S. Park, J. O. Baker, M. E. Himmel, P. A. Parilla, and D. K. Johnson, *Biotechnol. Biofuels,* **3**, 1 (2010).
27. T. Pullawan, A. N. Wilkinson, and S. J. Eichhorn, *Compos. Sci. Technol.,* **70**, 2325 (2010).
28. G. Sebe, F. Ham-Pichavant, E. Ibarboure, A. L. Chantal Koffi, and P. Tingaut, *Biomacromolecules,* **13**, 570 (2012).
29. M. Fan, D. Dai, and B. Huang, in "Fourier Transform - Materials Analysis" (Salih, Mohammed Salih Ed.), pp.45-

68, In Tech, 2012.
30. B. Stuart, "Infrared Spectroscopy: Fundamentals and Applications", pp.45-93, John Wiley & Sons, 2004.
31. J. X. Sun, F. Xu, X. F. Sun, B. Xiao, and R. C. Sun, *Polym. Degrad. Stabil.,* **88**, 521 (2005).
32. M. Brebu and C. Vasile, *Cell. Chem. Technol.,* **44**, 353 (2010).
33. P. Giudicianni, G. Cardone, and R. Ragucci, *J. Anal. Appl. Pyrolysis,* **100**, 213 (2013).
34. A. E. Ghaly and A. Ergudenler, *Appl. Biochem. Biotechnol.,* **28**, 111 (1991).